2018-3

Studies of Geometrical Profiling in Fabricated Tapered Optical Fbers Using Whispering Gallery Modes Spectroscopy

Vishnu Kavungal
d12127257@mydit.ie

Gerald Farrell
Technological University Dublin, gerald.farrell@tudublin.ie

Qiang Wu
Northumbria University, Newcastle upon Tyne NE1 8ST, United Kingdom, qiang.wu@northumbria.ac.uk

See next page for additional authors

Recommended Citation

Kavungal, V., Farrell, G., Wu, Q., Mallik, A. K., Semenova, Y. (2018) Studies of geometrical profiling in fabricated tapered optical fibers using whispering gallery modes spectroscopy. *Optical Fiber Technology*, Vol. 41, March 2018, Pages 82-88. doi.org/10.1016/j.yofte.2018.01.007

Studies of geometrical profiling in fabricated tapered optical fibers using whispering gallery modes spectroscopy

VISHNU KAVUNGAL[1*], GERALD FARRELL[1], QIANG WU[1,2], ARUN KUMAR MALLIK[1], AND YULIYA SEMENOVA[1]

[1]*Photonics Research Centre, Dublin Institute of Technology, Kevin St, Dublin, Ireland*
[2]*Department of mathematics, Physics and Electrical Engineering, Northumbria University, Newcastle upon Tyne, NE1 8ST, United Kingdom*

*Corresponding author: vishnu.kavungal@mydit.ie

This paper experimentally demonstrates a method for geometrical profiling of asymmetries in fabricated thin microfiber tapers with waist diameters ranging from ~10 to ~50 µm with submicron accuracy. The method is based on the analysis of whispering gallery mode resonances excited in cylindrical fiber resonators as a result of evanescent coupling of light propagating through the fiber taper. The submicron accuracy of the proposed method has been verified by SEM studies. The method can be applied as a quality control tool in fabrication of microfiber based devices and sensors or for fine-tuning of microfiber fabrication set-ups.

Keywords: *Fibers; Fiber optics sensors; Microcavity devices; Microstructured optical fibers; Resonators; Surface waves; Fiber characterization; Fiber properties.*

1. INDRODUCTION

Precise measurement of the outside diameter of standard optical fibers is important in both the manufacturing and quality control of such fibers. Fiber diameter measurements are used to understand and dynamically control the fiber drawing process and to select fibers suitable for commercial use. Other areas where a highly accurate fiber diameter measurement technique is required are related to improving the quality of fiber Bragg gratings [1], fabrication of special fibers, fiber-based devices, and more recently, microfiber based resonant devices [2].

Many of the fiber diameter measurement techniques developed to date are based on an analysis of interference fringes or diffraction patterns produced as a result of light scattering by an optical fiber under test [3-11]. The accuracy of these techniques is in the order of a few tens of nanometers, but complex equipment is required utilising spatial optics which involves complex measurement and signal processing. Birks et al. [12] suggested a simple and accurate method for the measurement of the variations in the diameter of an optical fiber based on the use of a microfiber. In their experiment, a guided mode of a microfiber was evanescently coupled into whispering-gallery modes (WGMs) propagating around the circumference of the fiber under test, which itself served as a cylindrical micro-resonator.

WGMs are electromagnetic surface oscillations which arise in dielectric micro-resonators with a circular structure as a result of the trapping of light within the micro-resonator by total internal reflections from the resonator's curved surface with a near-glancing incidence (angle of incidence (i) ~ 90°) [13]. Such reflections force the light to take on a polygonal path within the curved structure, very close to the surface of the resonator, and effectively confine its energy within very small volumes. The exceptional sensitivity of such resonances to the shape and size of the resonator make WGM spectroscopy a promising tool for geometrical profiling that can measure diameter variations at a sub-wavelength scale.

In Birks's experiments a microfiber with a guided light mode was used to accurately measure the relative diameter variations of less than one part in 10^4, as a possible means to implement accurate diameter control for fibre drawing. In that scheme, the microfiber and fibre under test moved relative to each other and were also in physical contact with each other. The fibre under test acted as a cylindrical WGM resonator and the fiber diameter variation was calculated from the shift of a WGM resonance detected in the transmission spectrum of the microfiber. This technique was further developed by Sumetsky and Dulashko in [14] by addressing some problems in Briks's method that arose because only a single resonance was tracked. This problem was resolved in Sumetsky's method by increasing the number of WGM resonances whose

spectral positions were traced leading to the demonstration of reliable angstrom fiber diameter measurement accuracy.

Another alternative method of fiber characterization is by calculating the effective diameter of the resonator using the information from the WGMs spectral spacing. The fundamental WGMs are localized close to the surface of the cylindrical resonator and thus the FSR can be linked to the microresonator's effective diameter [15, 16]. Using this approach, Boleininger et al. [17] experimentally demonstrated WGM profiling of a 3 mm long tapered optical fiber with a diameter >80 μm, and verified the accuracy of their method using optical microscopy data.

Tapered optical fibers themselves have been intensively studied in the recent years for applications as sensors for temperature, strain and biomedical measurands as well as various devices for optical communications due to their simple fabrication, configurability and excellent performance [2, 18-21]. More recently asymmetric fiber tapers have attracted a lot of attention as high sensitivity sensors, narrow-line optical comb filters [22-25] and surface nano-scale axial photonics devices [26-29]. The growing popularity of tapered fiber based devices requires the development of a simple and accurate taper profiling and a-/symmetries characterization method which would be useful for better understanding of such devices fabrication and quality control.

In this paper, we for the first time explore and experimentally demonstrate applicability of WGM spectroscopy for characterization of asymmetries in thin fiber tapers with waist diameters ranging from ~10 to ~50 μm where a submicron resolution is required.

Our WGM spectroscopy method is based on calculations of effective diameters using the experimentally measured FSR of the WGMs spectra. The technique is nondestructive and the measurements can be carried out *in situ* as opposed to measurements with an optical microscope. In addition, the proposed technique is a better alternative to optical microscopy since its resolution is not limited by the diffraction limit. To verify the submicron accuracy of our proposed method effective diameters of the tapered fibers calculated using the WGM spectroscopy were verified by scanning electron microscopy (SEM).

2. THEORETICAL BACKGROUND

(a) Tapered fiber transmission spectra.

The transmission characteristics of a tapered optical fiber, coupled with a cylindrical micro resonator and the coupled power circulating inside the cylindrical micro-resonator, can be described using universal coupled microcavity theory [30]. In Fig. 1, the field amplitudes at the input and output of the tapered optical fiber are denoted as a_1 and b_1 respectively.

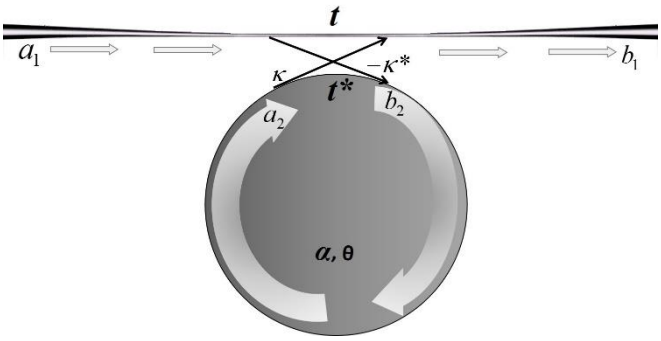

Figure 1. Schematic diagram of tapered fiber coupled cylindrical resonator.

The coupled field amplitudes in the cylindrical micro-resonator immediately before and after the coupling region are a_2 and b_2 respectively. The circulation loss factor inside the cylinder is denoted by α, which can be found from [30]:

$$\frac{a_2}{b_2} = \alpha e^{i\theta} \tag{1}$$

where θ is the circulation phase shift given by:

$$\theta = \frac{4\pi^2 R n_{eff}}{\lambda} \tag{2}$$

Here n_{eff} is the effective refractive index of the mode that propagates along a circular path within the cavity, R is the radius of the cylindrical micro-cavity, and λ is the resonance wavelength.

By setting $a_1 = 1$, the normalized transmission power of the tapered optical fiber is given by [30]:

$$|b_1|^2 = \frac{\alpha^2 - 2\alpha|t|\cos(\theta - \varphi_t) + |t|^2}{1 - 2\alpha|t|\cos(\theta - \varphi_t) + \alpha^2|t|^2} \tag{3}$$

Here t represents the transmission coefficient of the system, which is related to the coupling coefficient (κ) by the equation:

$$|t|^2 = 1 - |\kappa|^2 \tag{4}$$

where φ_t is the phase offset due to coupling to the tapered optical fiber. When the resonance condition is satisfied, φ_t is zero [31].

Based on Eq. (3), the typical curves of the loss factor (α) due to circulation versus transmission power for a cylindrical resonator-tapered fiber system are simulated and shown in Fig. 2 (a). The simulated plots are for three different values of $|t|$ equal to 0.999, 0.980, and 0.960 respectively. From Eq. (3) it can be seen that when $|t| = \alpha$, there is no light power in the transmission spectrum ($|b_1|^2 = 0$). This is due to the fact that when the internal loss is equal to the transmission loss there is a perfect destructive interference in the tapered fiber between the power transmitted through the fiber taper and the circulating power leaked from the cylindrical resonator. This condition is referred to as the critical coupling [30].

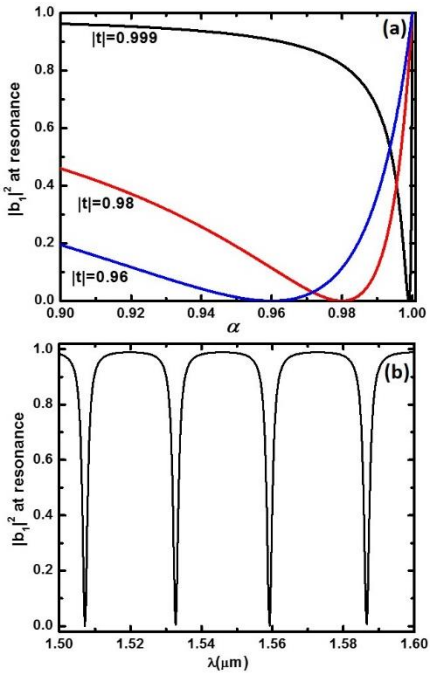

Figure 2. (a) Relationship between the transmission power of the tapered fiber coupled with the cylindrical microresonator with the resonator internal loss coefficient (α) and, transmission loss coefficient (|t|) with its transmission power. (b) The simulated transmission spectrum of the tapered fiber at critical coupling.

For illustration purposes, Fig. 2 (b) shows the simulated transmission spectrum of the tapered fiber (based on Eq. 3) coupled with a 20 μm diameter cylindrical micro resonator at critical coupling by setting both the cavity's internal loss coefficient (α) and the transmission loss coefficient (|t|) equal to 0.90.

(b) Effective radius of the resonator and the FSR of its WGM spectrum

A simple approximation can be obtained for the FSR from the propagation constant and neglecting the wavelength dependency of the refractive index [15, 16].
The light wave propagation constant is given by:

$$\beta(\lambda) = \frac{2\pi}{\lambda} n_{eff} \tag{5}$$

Differentiate Eq. (5) with respect to λ,

$$\frac{\partial \beta(\lambda)}{\partial \lambda} = -\frac{2\pi}{\lambda^2} n_{eff} + \frac{2\pi}{\lambda}\frac{\partial n_{eff}}{\partial \lambda}$$

$$\frac{\partial \beta(\lambda)}{\partial \lambda} = -\frac{2\pi}{\lambda^2}\left(n_{eff} - \frac{\partial n_{eff}}{\partial \lambda}\lambda\right) \approx \frac{-2\pi n_g}{\lambda^2} \tag{6}$$

where $n_g = n_{eff} - \frac{\partial n_{eff}}{\partial \lambda}\lambda$, is the group refractive index.

FSR of the resonator is given by the equation [29]:

$$FSR = \frac{-2\pi}{L}\left(\frac{\partial \beta}{\partial \lambda}\right)^{-1} = \frac{-2\pi}{L}\left(\frac{-\lambda^2}{2\pi n_g}\right) \approx \frac{\lambda^2}{n_g L} \tag{7}$$

where L is the circumference of the resonator.

It should be noted that the group refractive index varies with the change of the mode order. But for the lowest order modes this variation is small and can be neglected [16]. When calculating the FSR we are only considering the fundamental modes of the WGM spectrum, which have the lowest radial mode number. Hence neglecting the $\frac{\partial n_{eff}}{\partial \lambda}\lambda$ term from the expression for n_g, an approximate expression for the FSR is obtained as [15, 16]:

$$FSR = \frac{\lambda^2}{L n_{eff}} = \frac{\lambda^2}{2\pi R n_{eff}} \tag{8}$$

Eq. (8) represents the main approximation that underpins the approach presented in this paper. It assumes that the wavelength dependence of n_{eff} is negligibly small and the variation of the FSR of a resonator depends only on the micro-resonator radius.
As was shown in reference [32], Eq. (8) is not only useful for finding the spectral spacing between the modes within the uniform diameter portion of the resonator but can also be used for calculating the spectral spacing in the conical portion of the tapered fiber transition region.

3. EXPERIMENTS AND DISCUSSION

(a) Fabrication of tapered optical fibers

Light propagation inside a standard optical fiber with a diameter greater than the propagating light wavelength is based on total internal reflection where the light is trapped inside the core. When light hits the interface between the core and cladding layers, a small amount of the light infiltrates the boundary as an evanescent field that exponentially decays into the cladding region. The penetration depth of the evanescent field into the surrounding region is given by the relation [33]:

$$d_p = \frac{\lambda}{2\pi(n_1^2 \sin^2\Theta - n_2^2)^{1/2}} \tag{10}$$

Here λ is the wavelength of incident light, n_1 and n_2 are the refractive indices of the core and cladding respectively. Θ is the incident angle measured from the normal at the interface of the core and cladding. The reflected beam from the interface is returned to the core with a phase shift along its axial propagation direction.
When the diameter of a tapered optical fiber is greatly reduced, the original fiber core dimensions are so small at the waist region that they are no longer significant. In this case, an optical fiber can be considered as a cylindrical waveguide with a homogeneous refractive index profile. In a thin (micron order) fiber taper light is guided by the total internal reflection at the cladding-air interface (if the surrounding medium is air). Thus a significant portion of light propagates outside of the microfiber. The presence of a large evanescent field outside of the tapered portion of the fiber can be used for coupling the light into another fiber acting as the WGM micro-resonator by placing both fibers in direct physical contact.
A typical optical fiber taper consists of a non-tapered portion followed by a fiber taper transition region where the radius of the fiber decreases with distance. The uniform thin portion

after the transition region is known as the taper waist. This is followed by a second fiber transition region of increasing diameter and ends with another non-tapered region. The optical properties of the tapered micro-fibers strongly depend on the geometry of both the transition and waist regions. If the tapering process is carried out in such a way that the fiber diameter within its transition region changes smoothly and can be adiabatically slow as a function of fiber length, the taper is considered adiabatic [34, 35]. This condition ensures low transmission loss and small inter-mode coupling. In our experiments, only adiabatic tapers were studied.

The fiber tapers both for light coupling and as the microfibers under test, were fabricated using the micro-heater brushing technique [36, 37]. The technique involved stripping the coating off a short length of a standard single mode optical fiber (SMF 28, Corning), with core and cladding diameters of 8.3 and 125 μm respectively, and its subsequent cleaning with isopropyl alcohol. The stripped and cleaned fiber section was then fixed horizontally between two computer controlled XYZ translational stages. A ceramic micro heater (CMH-7019, NTT-AT) was used to heat the fiber up to approximately 1300°C, making the silica material soft enough for tapering. A customized PC program allowed for the control of the diameter, the length and the shape of the fabricated tapers. Figure 3 illustrates a schematic diagram of the fiber tapering setup.

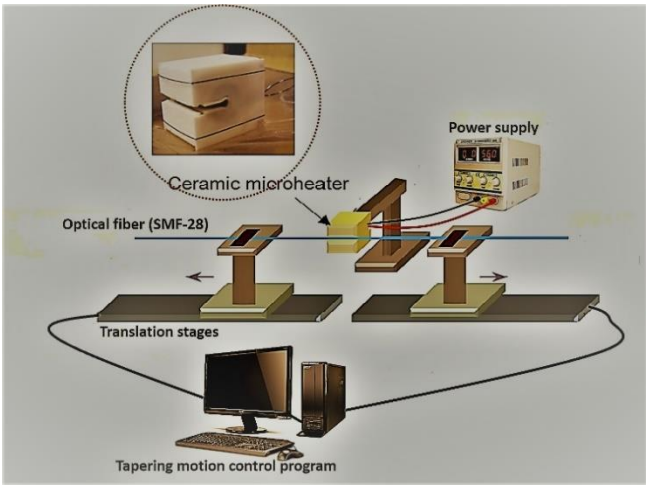

Figure. 3. Schematic diagram of the microfibre fabrication setup using the microheater brushing technique.

(b) Experimental set up for geometrical profiling of fabricated tapered optical fibers.

For geometrical profiling in our experiment a fiber taper under test was moved in small steps, in a manner similar to the technique described in [14], perpendicularly to a fixed "delivery" microfiber, the ends of which were connected to the optical source (SLD, Thorlabs) and the optical spectrum analyzer (86142B, Agilent) as shown in Figure 4. Both fibers were placed in physical contact at 90^o to each other so that the tapered fiber under test acted as a cylindrical WGM micro-resonator.

The fabricated fibers tested in our experiments were set to be fabricated with uniform taper waist diameters varying from ~10 to ~50 μm. The delivery microfiber had a waist diameter of circa ~1.3 μm. This value of the taper waist diameter was chosen as optimal to allow for an effective evanescent coupling while providing sufficient mechanical stability during the experiments.

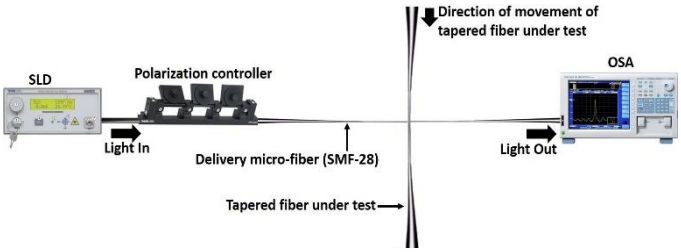

Figure 4. Schematic of the experimental setup for whispering gallery mode spectroscopy

Narrow WGM resonances are observed in the transmission spectrum of the delivery microfiber with a maximum *Q* factor of ~2.55 x 10^3 (for a 125 μm fiber/cylinder).

In the geometrical profiling experiment the transmission spectra of the light through the delivery microfiber was recorded for multiple positions of the "delivery" microfiber along the length of the taper under test with a step size of 0.5 mm along its axis. After each measurement, the fiber under test was lifted off the delivery fiber by approximately 1 mm, moved along the "delivery" fiber and placed in contact with it at the next point to take the subsequent measurement. This approach reduces the distortion of both the delivery fiber and the fiber under test and the possible damage from abrasion of the fiber surfaces. The FSR of the measured transmission spectrum is a function of the effective diameter of the tapered fiber under test (Eq. 8).

As an initial test, a recorded WGM spectrum for a micro-fiber cylindrical resonator with a known nominal 35.5 μm diameter was measured. Figure 5 shows the experimentally measured spectrum along with the theoretically calculated spectrum using Eq. 3. The experimental and simulated FSRs are estimated as 14.37 nm and 14.63 nm respectively for the 35.5 μm diameter micro-fiber resonator. Using Eq. (3) and assuming n_{eff} ≈1.4677 for the resonator from the manufacturers data, the corresponding effective diameter of the fiber under test from the experimental FSR is estimated as 36.28 μm. For the theoretical plot in Figure 5, the cavity loss and transmission loss are set as 0.9 and 0.86 respectively allowing to achieve a close fit for transmission loss between the theoretical and experimental spectra. The light circulation phase shift (θ) was calculated from Eq. (2).

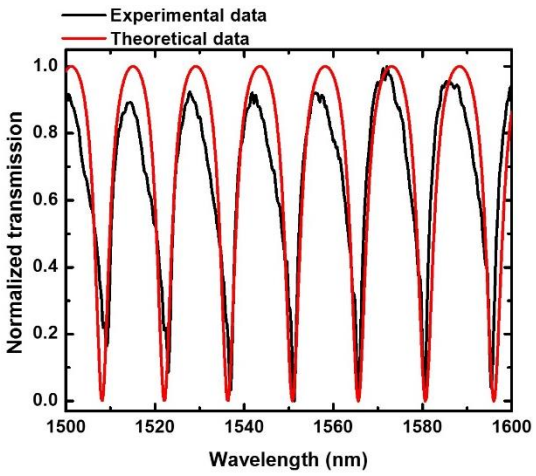

Figure 5. Experimental WGM spectrum of the delivery fiber and a simulated spectrum using Eq. 3.

(c) Geometrical profiling of optical fiber tapers

Before considering the experimental geometrical profiling results, it is worth noting that the shape of a tapered fiber is important and the requirements to the taper transition length, diameter of the uniform section and taper angle vary depending on the applications. For example, in many applications the fiber taper shape must be sufficiently gradual to satisfy the criterion for adiabaticity, so as to ensure minimum loss of light for the fundamental mode [38]. In some applications it is desirable for the transition region to be as short as possible, allowing the fiber taper to be compact. The shape of a taper is also important in situations where the taper is to be controllably deformed; for example, by bending, to fabricate miniature devices. Special shape considerations may also apply if the taper is to be used as a sensor. Many of the fiber tapering techniques developed to date allow for fabrication of the fiber tapers with specific shapes.

For the geometrical profiling experiments, two tapered fiber samples were used with nominal minimum waist diameters determined by SEM of ~11.2 µm (Taper 1) and 35.5 µm (Taper 2) respectively. SEM measurements were undertaken using a variable pressure FESEM (SU 6600) with a Schottky field emission electron gun which enables excess of 200 nA probe current. The attainable SEM image resolution is 1.2 nm/30 kV. Figure 6 shows the SEM images of the minimum waist sections for the two tapered fiber samples.

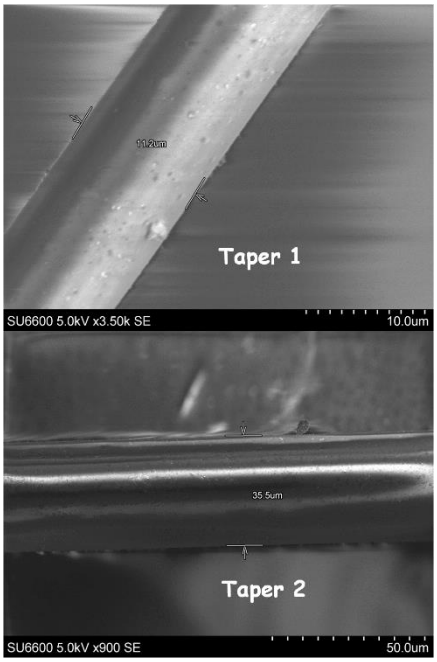

Figure 6. SEM images of the uniform waist portions of the tapered optical fibers.

Figure 7 shows the FSR and measured diameter versus position of the delivery fiber for the two tapered fiber samples. The minimum waist diameters recorded are estimated as 10.43 µm and 36.28 µm, taken at position zero in Figure 7.

Table 1 shows the comparison between different fiber diameter measurements using WGM spectroscopy and SEM microscopy. The maximum error between the two measurements methods is 0.77 µm (6.8 %). The disparity between nominal diameters (measured from a SEM image) and the experimentally measured diameters may be due for example to inaccuracies in the SEM determined diameter of the resonator under test or small variations in actual position of the delivery tapered fiber and the tapered fiber under test.

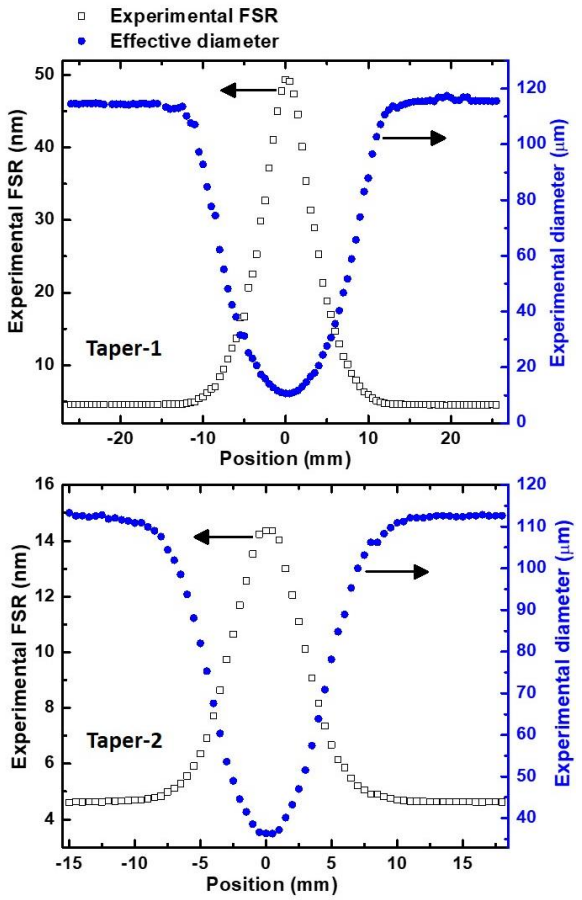

Figure 7. Experimentally calculated FSR and diameter vs position of the delivery fiber for a taper with a nominal waist diameters of 11.2 μm (Taper 1) and 35.5 μm (Taper 2) measured by WGM spectroscopy. Zero position corresponds to the center of the taper.

Table 1. Comparison of measured fiber diameter using WGMs and SEM microscopic methods

(a) Diameter (μm) from WGM Spectroscopy	(b) Diameter (μm) from SEM microscopy	(a)-(b) Error (μm)
48.66	48.4	0.26 (0.54 %)
45.51	45.6	0.09 (0.2 %)
38.52	38.8	0.28 (0.72 %)
36.26	35.5	0.76 (2.1 %)
10.43	11.2	0.77 (6.8 %)

It should be noted that profiling of the tapered fibers using WGM spectroscopy allows one to easily obtain accurate information not just about the taper effective diameter at a certain point but also to fully evaluate the shape of the taper along its length and determine the lengths of the taper transition regions and the uniform tapered portion. For example, from Figure 7 it can be determined that Taper 1 has transition regions 11 mm long on the left-hand side and 10 mm long on the right-hand side and that the uniform tapered portion is about 3.5 mm long. Taper 2 has transition region lengths of 9.5 mm and 10 mm on the left and right-hand sides respectively and the uniform tapered portion is about 2.5 mm long.

(d) Application of the WGM spectroscopy to studies of taper symmetry

In an ideal case, a fiber taper is formed symmetrically. This means that the ends of the taper are pulled apart at equal and opposite speeds relative to the center of the heat source so that the two transition regions are identical. In practice however various factors, such as misalignments within the tapering setup, vibration or temperature fluctuations within the heating zone of the source may result in uneven conditions at the opposite sides of the taper and lead to asymmetries of the fiber taper shape. One important parameter in the model of the fiber tapering process developed in [38] is the constant which determines the relative rates of the hot-zone change and taper elongation Ψ[1] the value of Ψ must satisfy the condition $\Psi \leq 1$ and it determines the length of the uniform waist region along with the shape of the transition regions.

To provide a set of non-ideal tapers for test purposes, a fabrication configuration was used that was known to produce increasingly asymmetrical tapers for larger Ψ values, due to mechanical limitations caused by vibration. This setup, although flawed in principle, was deliberately used to fabricate non-ideal tapers for testing of the WGM spectroscopy method presented here.

Figure 8 (a) illustrates the experimental WGM spectroscopic profiles of a highly asymmetric taper (Taper-3) fabricated using the above mentioned setup. Figure 8 (b) shows the comparison of the fabricated asymmetric taper with a symmetric taper, in this case Taper-2. Both fiber tapers were fabricated using the same fabrication unit with different configurations. The symmetrical Taper-2 is fabricated by setting the Ψ - parameter to zero ($\Psi = 0$). Since Taper-2 has the smaller Ψ value, it is expected to be close to symmetrical. Thus, the two transition regions should have almost the same length. Taper-3 is fabricated by setting Ψ to 1 and because of the larger Ψ value is expected to have a more asymmetrical profile. The estimated minimum waist diameters are ~36.26 μm as before for Taper-2, and ~41.7 μm for Taper-3. From inspection of Figure 8 (b) the waist region of Taper-3 is much

[1] In the original reference paper (Ref [38]), the constant which determines the relative rates of the hot-zone change and taper elongation is represented by 'α'. To avoid the possibility of confusion with the previously used symbol for circulation loss factor inside the micro-cylinder, here we are using Ψ instead of α

less uniform and it is clear the left and right hand-side transition regions have very different lengths.

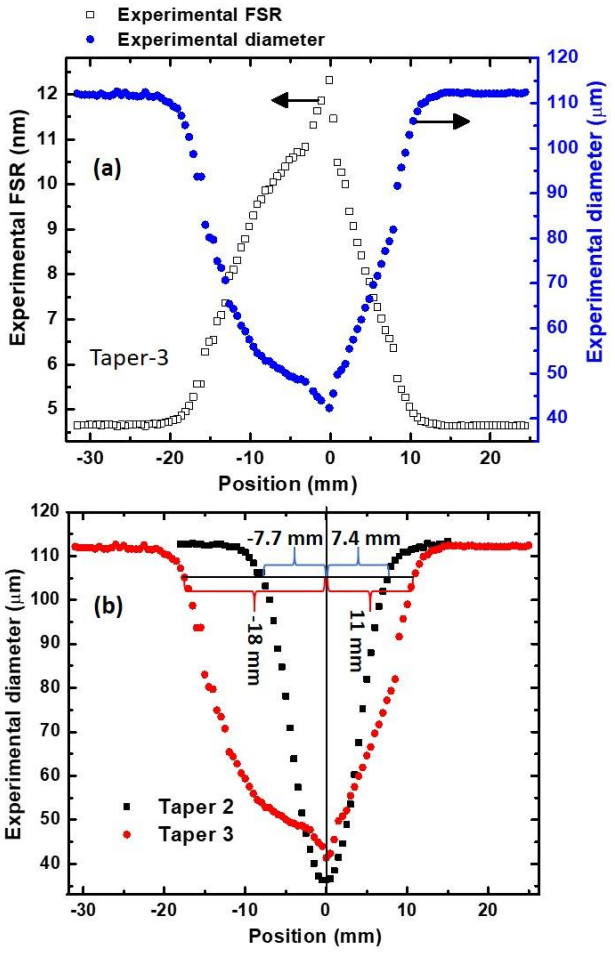

Figure 8. (a) FSR and experimental diameter vs position of the delivery fiber for an asymmetrical taper with a minimum waist region effective diameter ~ 41 μm. The experimental diameter is calculated by the WGM spectroscopy method. (b) Comparison of two experimental profiles for tapered optical fibers drawn under different conditions.

In order to systematically examine the measured asymmetry, a detailed comparison of the symmetric (Taper-2) and asymmetric taper (Taper-3) profiles is shown in Figure 9. Here the horizontal axis represents the distance from the center of the uniform waist region towards left and right-hand side transition regions of the fiber tapers. The vertical axis illustrates the corresponding experimental diameter of the tapered region. From Figure 9, the profiles for the left and right-hand sides of Taper-2 almost overlap, indicating a high degree of symmetry. Taper-3 on the other hand is highly asymmetrical. Both the left and right-hand side transition regions are at maximum 7 mm apart with respect to the center of the uniform waist. The lengths of the transistions regions are 12.5 mm and 9.5 mm.

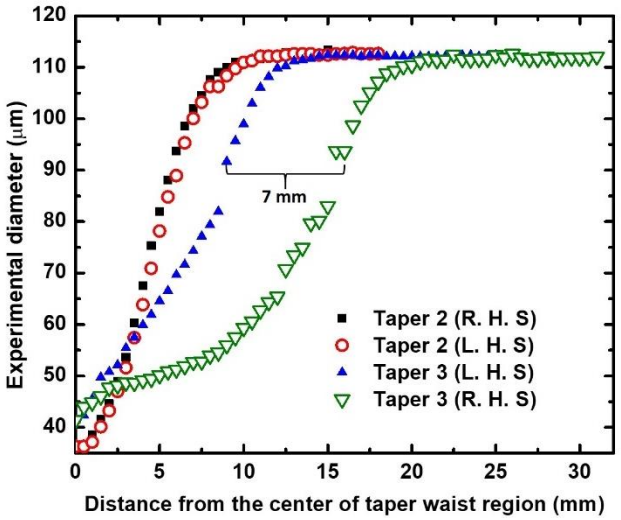

Figure 9. Comparison of variation in left and right-hand side transition regions of a symmetrical and an asymmetrical fiber taper.

The proposed method of diameter profiling requires accurate calculation of an FSR of the WGM spectrum within the wavelength range determined by the bandwidth of the broadband source used in the experiment. For the calculation of the spectrum's FSR, at least two WGM resonances must be observable in the given wavelength range, and since the FSR of a WGM spectrum is inversely proportional to the microresonator's diameter, the minimal measurable diameter is limited by the bandwidth of the optical source. In our experiment the broadband superluminescent diode source had a bandwidth of 1500-1600 nm, resulting in a minimal measurable diameter of the cylindrical microresonator of 6 μm.

4. CONCLUSIONS

In conclusion, we have experimentally demonstrated a method for geometrical profiling of thin microfiber tapers with waist diameters ranging from ~10 to ~50 μm with submicron accuracy. The method is based on the analysis of WGM resonances excited in cylindrical fiber resonators as a result of evanescent coupling of light propagating through the fiber taper under test. Tapered fibers with different shapes were fabricated deliberately to demonstrate the capabilities of the proposed method. It has been demonstrated that the proposed method allows for investigation of the tapers' symmetry and the length of the uniform waist region. Measurement results have been verified by SEM microscopy with a maximum error of 0.77 μm. The proposed method can be applied in fabrication of fiber micro tapers as the means of accurate feedback of the taper diameter as a less expensive alternative with similar accuracy to microscopic measurements. It can also be used to detect flaws in a taper fabrication setup. Finally, the method could also be potentially applied to sensing of biochemical species on the surface of the microfiber, where the effective diameter and

refractive index of the resonator fiber can be increased due to adsorption of biochemical species on the fiber surface.

Acknowledgement

Authors would like to acknowledge the support of Dublin Institute of Technology and DIT Fiosraigh Scholarship Program

REFERENCES

[1]. M. Ibsen and R. I. Laming, in *Optical fiber Communication Conference* (Optical Society of America, 1999), paper FA1.

[2]. L. Tong, M. Sumetsky, Subwavelength and Nanometer Diameter Optical Fibers (Zhejiang University Press & Springer, 2009)

[3]. D. H. Smithgall, L. S Watkins and R. E. Frazee Jr, "High-speed noncontact fiber-diameter measurement using forward light scattering", Appl. Opt. 16, (1977) 2395-2402.

[4]. J. F. Owen, P. W. Barber, B. J. Messinger, and R. K. Chang, "Determination of optical-fiber diameter from resonances in the elastic scattering spectrum", Opt. Lett. 6, (1981) 272-274.

[5]. M. Young, P. D. Hale, and S. E. Mechels, "Optical fiber geometry: Accurate measurement of cladding diameter", J. Res. Natl. Inst. Stand. Technol. 98, (1993) 203-215.

[6]. E. Frins, H. Failache, J. Ferrari, G. D. Costa, and A. Lezama, "Optical-fiber diameter determination by scattering at oblique incidence", Appl. Optics. 33, (1994) 7472-7476.

[7]. J. C. Knight, H. Steve T. Driver, G. N. Robertson, "Measurement of capillary core size and taper using whispering-gallery-mode laser emission", Opt. Engineering. 33, (1994) 2838-2842.

[8]. M. B. van der Mark, and L. Bosselaar, "Noncontact calibration of optical fiber cladding diameter using exact scattering theory", J. Light wave. Tech. 12, (1994) 1-5.

[9]. A. W. Poon, and R. K. Chang, D. Q. Chowdhury, "Measurement of fiber-cladding diameter uniformity by use of whispering -gallery modes: nanometer resolution in diameter variations along millimeter to centimeter lengths", Opt. Lett. 26, (2001) 1867-1869.

[10]. J. Jasapara, E. Monberg, F. DiMarcello, and J. W. Nicholson, "Accurate noncontact optical fiber diameter measurement with spectral interferometry", Opt. Lett. 28, (2003) 601-603.

[11]. F. Warken and H. Giessen, "Fast profile measurement of micrometer-sized tapered fibers with better than 50-nm accuracy", Opt. Lett. 29, (2004) 1727-1729.

[12]. T. A. Birks, J. C. Knight and T. E Dimmick, "High-Resolution Measurement of the Fiber Diameter Variations Using Whispering Gallery Modes and No Optical Alignment", IEEE Photon. Technol. Lett. 12, (2000) 182-183.

[13]. G. C. Righini. Y. Dumeige, P. Feron, M. Ferrari, G. N. Conti, D. Ristic, and S. Soria, "Whispering gallery mode microresonators: Fundamentals and applications" Rivista Del Nuovo Cimento. 34, (2011) 435-488.

[14]. M. Sumetsky and Y. Dulashko, "Radius variation of optical fibers with angstrom accuracy", Opt. Lett. 35, (2010) 4006-4008.

[15]. W. Bogaerts, P. D. Heyn, T. V. Vaerenbergh, K. D. Vos, S. K. Selvaraja, T. Claes, P. Dumon, P. Bienstman, D. V. Thourhout, and R. Baets, "Silicon microring resonators", Laser Photonics Rev. 6, (2012) 47-73.

[16]. D. G. Rabus, Integrated Ring Resonators, Springer series in Optical Sciences, Chapter 2, 2007, p.127.

[17]. A. Boleininger, T. Lake, S. Hami and C. Vallance, "Whispering Gallery Modes in Standard Optical Fibres for Fibre Profiling Measurements and Sensing of Unlabelled Chemical Species", Sensors, 10, (2010) 1765-1781.

[18]. Y. Tian, W. Wang, N. Wu, X. Zou, and X. Wang, "Tapered optical fiber sensor for label-free detection of biomolecules", Sensors 11, (2011) 3780-3790.

[19]. H. Y. Lin, C. H. Huang, G. L. Cheng, N. K. Chen, and H. C. Chui, "Tapered optical fiber sensor based on localized surface plasmon resonance", Opt. Express. 20, (2012) 21693-21701.

[20]. C. Bariáin, I. R. Matías, F. J. Arregui, M. López-Amo, "Optical fiber humidity sensor based on a tapered fiber coated with agarose gel" Sensors and Actuators B: Chemical 69, (2000) 127-31.

[21]. W. Jin, H. L. Ho, Y. C. Cao, J. Ju, L. F. Qi, "Gas detection with micro-and nano-engineered optical fibers" Optical Fiber Technology. 19, (2013) 741-759.

[22]. N. H. Mohamed Halip, N. S. Isa, A. A. Latif, M. A. Mahdi, M. H. Abu Bakar, "Asymmetric fiber taper for narrow linewidth comb filter" Jurnal Teknologi. 78.3, (2016) 117-121.

[23]. M. Deng, D. Liu, D. Li, "Magnetic field sensor based on asymmetric optical fiber taper and magnetic fluid", Sensor and Actuators A: Physical. 211, (2014) 55-59.

[24]. R. Radzali, Y. Mustapha Kamil, M. A Mahdi, M. H. Abu Bakar, "Asymmetric fiber taper for temperature sensing applications" 2015 IEEE International broadband and photonics conference, Bali, (2015) 23-25.

[25]. C. L. Lee, W. C. Shih, J. M. Hsu, and J. S. Horng, "Asymmetrical dual tapered fiber Mach-Zehnder interferometer for fiber-optic directional tilt sensor", Opt. Express. 22, (2014) 24646- 24654.

[26]. M. Sumetsky, D. J. DiGiovanni, Y. Dulashko, J. M. Fini, X. Liu, E. M. Monberg, and T. F. Taunay, "Surface nanoscale axial photonics: robust fabrication of hihg-quality-factor microresonators", Opt. Lett. 36, (2011) 4824-4826.

[27]. M. Sumetsky, K. Abedin, D. J. DiGiovanni, Y. Dulashko, J. M. Fini, E. Monberg, "Coupled high Q-factor surface nanoscale axial photonics (SNAP) microresonators", Opt. Lett. 37, (2012) 990-992.

[28]. M. Sumetsky, "Theory of SNAP devices: basic equations and comparison with the experiment"Opt. Express. 20, (2012) 22537-22554.

[29]. M. Sumetsky and J. M. Fini, "Surface nanoscale axial photonics", Opt. Express. 19, (2011) 26470-26485.

[30]. A. Yariv, "Universal relations for coupling of optical power between microresonators and dielectric waveguides" Electronic. Lett. 36, (2000) 321-322.

[31]. X. Zhang, T. Liu, J. Jiang, K. Liu, Z. Yu, M. Feng, W. Liu, and W. Chen, “Ultraprecise resonance wavelength determination for optofluidic sensing applications”, IEEE Photon. Technol. Lett. **27**, (2015) 399-402.

[32]. Ya. V. Alekseenko, A. M. Monakhov, and I. V. Rozhanskii, "Whispering Gallery Modes in a Conical Resonator" Tech. Phys. 54, (2009) 1633-1638.

[33]. M. Ahmad, L. L. Hench, "Effect of taper geometries and launch angle on evanescent wave penetration depth in optical fibers", Biosensors and Bioelectronics. 20, (2005) 1312-1319.

[34]. Harper, Kevin R., Timothy E. Dimmick, and Theodore E. Dubroff. "Tapered optical fibers." U.S. Patent Application No. 11/473,689.

[35]. M. Sumetsky, "How thin can a microfiber be and still guide light?", Opt. Lett. 31, (2006) 870-872.

[36]. G. Brambilla, V. Finazzi, and D. Richardson, "Ultra-low-loss optical fiber nanotapers," Opt. Express. 12, (2004) 2258-2263.

[37]. L. Bo, P. Wang, Y. Semenova, G. Farrell, "Highly-sensitive fiber refractometer based on an optical microfiber coupler," IEEE Photonics Tech. Lett. 25, (2013) 228-230.

[38]. T. A. Birks and Y. W. Li, "The shapes of fiber tapers", J. Lightwave Technol. 10, (1992) 432-438.